Title

A novel murine model for contact lens wear reveals clandestine IL-1R dependent corneal parainflammation and susceptibility to microbial keratitis upon inoculation with Pseudomonas aeruginosa

Journal

The Ocular Surface, 17(1)

ISSN

1542-0124

Authors

Metruccio, Matteo ME
Wan, Stephanie J
Horneman, Hart
et al.

Publication Date

2019

DOI

10.1016/j.jtos.2018.11.006

Peer reviewed

HHS Public Access

Author manuscript

Ocul Surf. Author manuscript; available in PMC 2020 January 01.

Published in final edited form as:

Ocul Surf. 2019 January ; 17(1): 119–133. doi:10.1016/j.jtos.2018.11.006.

A novel murine model for contact lens wear reveals clandestine IL-1R dependent corneal parainflammation and susceptibility to microbial keratitis upon inoculation with *Pseudomonas aeruginosa*

Matteo M. E. Metruccio[1], **Stephanie J. Wan**[2], **Hart Horneman**[1], **Abby R. Kroken**[1], **Aaron B. Sullivan**[1], **Tan N. Truong**[1,2], **James J. Mun**[1,#], **Connie K. P. Tam**[1,†], **Robin Frith**[3], **Laurence Welsh**[3], **Melanie D. George**[4], **Carol A. Morris**[4], **David J. Evans**[1,5], and **Suzanne M. J. Fleiszig**[1,2,6,*]

[1]School of Optometry, University of California, Berkeley, CA 94720, USA

[2]Graduate Group in Vision Science, University of California, Berkeley, CA 94720, USA

[3]CooperVision UK R & D Facility, Chandlers Ford, Eastleigh, Hants, SO534LY, UK

[4]CooperVision, Inc., Advanced Development Center, Pleasanton, CA 94588, USA

[5]College of Pharmacy, Touro University California, Vallejo, CA 94592, USA

[6]Graduate Groups in Microbiology, and Infectious Diseases & Immunity, University of California, Berkeley, CA 94720, USA

Abstract

Purpose—Contact lens wear carries a risk of complications, including corneal infection. Solving these complications has been hindered by limitations of existing animal models. Here, we report development of a new murine model of contact lens wear.

Methods—C57BL/6 mice were fitted with custom-made silicone-hydrogel contact lenses with or without prior inoculation with *Pseudomonas aeruginosa* (PAO1-GFP). Contralateral eyes served as controls. Corneas were monitored for pathology, and examined *ex vivo* using high-magnification, time-lapse imaging. Fluorescent reporter mice allowed visualization of host cell membranes and immune cells. Lens-colonizing bacteria were detected by viable counts and FISH. Direct-colony PCR was used for bacterial identification.

Results—Without deliberate inoculation, lens-wearing corneas remained free of visible pathology, and retained a clarity similar to non-lens wearing controls. CD11c-YFP reporter mice revealed altered numbers, and distribution, of CD11c-positive cells in lens-wearing corneas after

[*]Correspondence. School of Optometry, University of California, Berkeley, CA 94720-2020, USA. Tel. 1 (510) 643–0990, Fax. 1 (510) 643–5109. fleiszig@berkeley.edu.

[#]Present address. Johnson and Johnson, Inc., 33 Technology Drive, Irvine CA 92618, USA

[†]Present address. Cole Eye Institute. Cleveland Clinic. Cleveland, OH 44195, USA

24 h. Worn lenses showed bacterial colonization, primarily by known conjunctival or skin commensals. Corneal epithelial cells showed vacuolization during lens wear, and after 5 days, cells with phagocyte morphology appeared in the stroma that actively migrated over resident keratocytes that showed altered morphology. Immunofluorescence confirmed stromal Ly6G-positive cells after 5 days of lens wear, but not in MyD88 or IL-1R gene-knockout mice. *P. aeruginosa*-contaminated lenses caused infectious pathology in most mice from 1 to 13 days.

Conclusions—This murine model of contact lens wear appears to faithfully mimic events occurring during human lens wear, and could be valuable for experiments, not possible in humans, that help solve the pathogenesis of lens-related complications.

Keywords

Murine contact lens; parainflammation; IL-1R; CD11c-positive cells; Ly6G-positive cells; neutrophils; *Pseudomonas aeruginosa* keratitis

1. Introduction

Contact lenses represent a common form of vision correction with over 40 million wearers in the USA [1], and estimates of over 140 million wearers worldwide [2,3]. Lens-wear is expected to rise dramatically over the next decade due to an ongoing myopia epidemic [4], the use of lenses for drug delivery [5,6], development of lenses with biosensing electronics (health monitoring) [7,8], and their potential use for augmented reality [9].

It is well established, however, that contact lens wear can predispose the human cornea to various complications. The most serious is microbial keratitis [2,10] for which there are multiple risk factors; including microbial contamination of lenses and lens cases, overnight or extended wear, potential failure of lens care solutions, and poor hygienic practices [11–15]. Contact lenses also carry the risk of other corneal and ocular complications, including acute and chronic inflammatory events, dryness, and overall discomfort [2,3,16]. Unfortunately, despite considerable progress in contact lens design (e.g., development of silicone hydrogel lenses with high oxygen transmissibility), the incidence of microbial keratitis has not changed [17]. User non-compliant practices remain widespread, often under-reported, and may exacerbate the risk of adverse events [13,18–20]. The etiology and pathogenesis of infections, and other complications, remain unresolved.

Human studies, such as those cited above, are of considerable value in determining the epidemiology of contact lens-related complications, and risk factors involved. However, our progress in understanding these complications at a molecular, cellular, and tissue level has been hindered by the limitations of experiments that can be performed on human subjects

Several studies have reported the use of contact lens-wearing animal models to investigate the pathogenesis of lens-associated microbial keratitis. Examples include cytokine and chemokine profiles of *P. aeruginosa*-challenged corneas in a lens-wearing rat model [21,22], the association of contact lens-associated biofilms/bacterial adaptations in development of *P. aeruginosa* keratitis in a lens-wearing rat model [23], the relationship between neutrophil infiltration and severity of *P. aeruginosa* keratitis in a rabbit model [24], and the role of lens

colonization and microbial antigens in lens-induced infiltrative events in a guinea pig model [25]. However, these previous lens-wearing models have been limited by one or more factors: 1) limited lens supply [23], 2) use of a larger animal (e.g. rabbit) for which eyelid closure or nictitating membrane surgery is required for lens retention [24,26], 3) infiltrative, inflammatory events that occur but do not lead to microbial keratitis (e.g. guinea pig) [25], 4) microbial keratitis that does not occur or is evident at a low level despite repeated bacterial inoculation (e.g. rat) [21,22]. All of these models are also limited by availability of research tools suitable for the animals involved, such as methods for genetic manipulation and analysis, antibodies for protein detection, purification, or imaging, given that many modern reagents are designed for use only in mice.

In the absence of a mouse contact lens, researchers interested in understanding the pathogenesis of contact lens-induced infection have had to use surrogate models to ask relevant questions, including *in vitro* cell culture models. Other researchers have used *in vivo* mouse models in which scarification, healing after scarification, or intrastromal injection are used to induce infection. The latter have enormously advanced our understanding of the immune and inflammatory response to microbes [27–29], and the role of bacterial virulence factors [30–34], once infection has already initiated. However, while full-thickness epithelial injury is a common predisposing factor for corneal infection in non-lens wearers [35,36], there is little evidence to support the idea that contact lens wearers are predisposed to microbial keratitis in this way. Thus, such injury-based models are not ideal for exploring host and microbial factors involved in initiating infection of a previously healthy cornea in the context of contact lens wear.

Dendritic (or Langerhans) cell recruitment in the central cornea and conjunctiva has been reported as a response to contact lens wear in humans, regardless of material, solution type or lens wear modality [37–39]. Even though the cornea is normally devoid of resident viable bacteria [40], commensal microbe accumulation on human lenses during wear without resulting infection has also been well established [41]. Here, we report development of a novel contact lens-wearing murine model which faithfully reproduces both of these human events. Moreover, aligning with the known risk of infection with opportunistic microbes during human lens wear, corneas of mice wearing lenses became susceptible to infection with *P. aeruginosa*, an opportunist unable to infect healthy corneas in the absence of lens wear. Using reagents available for mice but not humans, we additionally show that uninoculated contact lens wear can induce parainflammation consisting of neutrophil recruitment in otherwise healthy-appearing corneas. This phenomenon was found dependent on MyD88 and IL-1R, well known for their role in host innate defense, and as we have previously shown, regulate multiple relevant phenomena in the healthy cornea including its lack of a viable bacterial microbiome, its glycosylation, and epithelial defenses against microbial adhesion and penetration [40,42,43]. This model allows us to further our understanding of lens-associated events at the ocular surface, and their role in susceptibility to infection. Such in-depth biochemical, tissue and cellular experiments involving use of molecular markers would not be possible in humans.

2. Methods

2.1 Murine contact lenses

The contact lenses used in this study were fabricated by CooperVision, Inc. (Pleasanton, CA) and were provided without compensation under a material transfer agreement between CooperVision, Inc. and the University of California, Berkeley. The lenses were custom-designed with parameters suited to fit the eyes of C57BL/6 mice, a challenging task due to the steep curvature of murine eyes, e.g. measurements of 6 weeks old C57BL/6 mice indicated a corneal diameter of 3.2 mm and SAG (Sagittal Depth) of 1.5 mm. The lens design was based upon fitting mouse corneas with those dimensions. Success of the design was shown by the excellent fit observed (see results). The mouse lenses are ~20 % of the average diameter of a human contact lens with a similar center thickness (e.g. maximum 0.70 mm). The lens material is the same as that of a currently marketed silicone hydrogel lens. However, these lenses are investigational devices, and may not be representative of, nor comparable to, any commercial contact lens product sold by CooperVision, Inc.

2.2 Murine model of lens wear

All procedures involving animals were carried out in accordance with standards established by the Association for the Research in Vision and Ophthalmology, under the protocol AUP-201608–9021 approved by the Animal Care and Use Committee, University of California Berkeley, an AAALAC accredited institution. The protocol adheres to PHS policy on the humane care and use of laboratory animals, and the guide for the care and use of laboratory animals. Wild-type C57BL/6 mice were used along with gene knockouts in MyD88 (−/−) or IL-1R (−/−). For imaging purposes, some experiments utilized mice with CD11c-YFP (CD11c-positive cells, e.g. dendritic cells, yellow), td-tomato or mT/mG (all cell membranes, red), or LysMcre (Lyz2-positive cells, myeloid-derived, green). Male and female mice were used, and all mice were obtained from the Jackson Laboratory (Bar Harbor, ME) except for F1 derived from the cross of mT/mG with either CD11c-YFP or LysMcre. The custom-made silicon hydrogel contact lenses were removed from their packaging solution and placed in sterile phosphate-buffered saline (PBS) for 1 h. A contact lens was then fitted to one eye of each mouse. A Handi-Vac suction pen (Edmund Optics, Barrington, NJ) with a 3/32” probe was used for contact lens handling and fitting (Supplemental Video S1) which was performed under isoflurane anesthesia (1.5 – 2 %) delivered using a precision vaporizer (VetEquip Inc., Pleasanton, CA). After lens application, mice were fitted with Elizabethan collars (Kent Scientific), then single-housed without enrichments to prevent lens removal using Pure-o’Cel paper bedding (The Andersons Inc., Maumee OH) to reduce dust levels. Mice were monitored daily for the retention of lenses, and evidence of pathology, e.g. discharge or corneal opacity, was recorded *via* stereomicroscope examination (Zeiss, Stemi 2000-C) with attached Canon EOS T5i camera while mice were under short-term (~ 20 min) isoflurane anesthesia. At the end of each experiment, or if mice presented with excessive weight loss, distress or signs of keratitis, euthanasia was performed using CO_2 asphyxia followed by cervical dislocation. Eyes were then enucleated for further experiments.

2.3 Confocal imaging

Freshly enucleated eyes were washed once in PBS, mounted upright on acrylamide adhesive and immersed in clear DMEM. Confocal imaging was performed using a 60×/1.00 NA or a 20×/0.56 NA water-dipping objective, and an upright Olympus Fluoview FV1000 Confocal Microscope. Eyes were imaged using 559 nm (td-tomato membrane), 515 nm (CD11c-YFP), and 488 nm (PAO1-GFP or $Lyz2^+$-GFP) laser lines. Z stacks (0.5 or 1 μm steps) were collected from 4 or more random fields per sample. In some experiments, Z-stacks over time were collected to capture moving cells. 3-D and 4-D image reconstruction, cell morphology analysis and movie generation were performed using Image-J (MorpholibJ tools collection) and Imaris (Bitplane). Maximum intensity projection (reducing a 3-D image into 2-D by projecting the maximum intensity of each pixel in a specific channel to the z plane) was used where indicated to visualize $Lyz2^+$ or $CD11c^+$ cell number and morphology, and to reduce 4D acquisition (xyz over time) in 2D movies (xy over time) to lower image complexity and better appreciate cell movement.

2.4 Immunofluorescence imaging

Freshly enucleated eyes were fixed in 2 % paraformaldehyde in PBS at 4 °C for ~16 h. Fixed eyes were then protected by immersion in sucrose (15 % for 4 h, then 30 % for an additional 4 h) at room temperature. Cryo-protected eyes were embedded in OCT (Tissue Tek), flash frozen in liquid nitrogen and stored at −80 °C. Embedded eyes were sectioned at 10 μm thickness using a Leica CM 1900 cryostat, placed on a glass slide and stored at −80 °C. Corneal sections were stained for Ly6G-positive cells using rat NIMP-R14 antibody (10 μg/mL, ThermoFisher) and Alexa 647-conjugated goat anti-rat antibody (5 μg/mL, Life Technology). Samples were counterstained with DAPI (12.5 μg/mL, ThermoFisher) and, in the case of sections from IL-1R (−/−) and MyD88 (−/−) mice, ActiGreen (Phalloidin, 1:10, ThermoFisher). Frozen sections were rinsed with PBS, blocked with 2 % BSA blocking buffer for 1 h, followed by primary antibody incubation for 1 h (both at room temperature). The sections were rinsed with PBS then incubated with secondary antibody for 1 h (also at room temperature), then rinsed with PBS, and mounted on a coverslip with Prolong Diamond (ThermoFisher). Sections were allowed to set for a minimum of 30 min before imaging using a Nikon Ti-E inverted wide-field fluorescence microscope equipped with Lumencor SpectraX illumination source, and CFI Plan APO VC 20×/0.75 NA objective. Neutrophil quantification was performed by manual counting $Ly6G^+$ cells in at least 4 fields per sample, and at least 3 samples per condition.

2.5 Bacteria

Pseudomonas aeruginosa strain PAO1 was used throughout. For many imaging experiments, PAO1 transformed with plasmid pSMC2 expressing enhanced GFP was used [44]. Bacteria were grown on tryptic soy agar (TSA) plates at 37°C for ~16 h. TSA was supplemented with carbenicillin 300 μg/mL for growing PAO1-GFP. Inocula were prepared by suspending bacteria in PBS to a concentration of ~10^7 CFU/mL (confirmed by viable counts). New contact lenses were then placed in the bacterial suspension for ~16 h at room temperature before fitting on the murine corneas. To ascertain the typical inoculum under these conditions, control experiments were performed in which new murine contact lenses were

inoculated with *P. aeruginosa* as above, and after ~16 h incubation at room temperature, viable counts were performed on lens homogenates. These inoculum preparation conditions reliably produced ~ 10^5 CFU/lens.

2.6 Bacterial isolation and identification

To culture bacteria from worn murine contact lenses, lenses were removed with sterile forceps, cut in half with a sterile scalpel, and placed in 500 μL of PBS in tubes containing 2.8 mm ceramic beads (Omni International). Samples were homogenized, plated onto TSA, and incubated at 37 °C in both aerobic and anaerobic conditions for up to 7 days. Isolated bacterial colonies were then identified by direct colony PCR of the 16S ribosomal RNA gene using universal primers P11P (5'-GAGGAAGGTGGGGATGACGT-3' and P13P (5'AGGCCCGGGAACGTATTCAC-3' [45]. Reaction mixes (50 μL) were set up as follows: 1× Q5 Reaction Buffer (New England BioLabs), 1× Q5 High GC Enhancer, 200 μM dNTPs, 0.5 μM Forward Primer, 0.5μM Reverse Primer, and 0.02 U/μL Q5 High-Fidelity DNA Polymerase. A sterile toothpick was used to touch a bacterial colony on an agar plate and inserted directly into the PCR reaction tube. The reaction mixtures were subjected to the following thermal cycling sequence on a Bio-Rad Thermal Cycler: 98 °C for 3 min followed by 30 cycles of 98 °C for 10 sec, 63 °C for 20 sec, 72 °C for 45 sec, followed by a final extension of 72 °C for 2 min. Molecular grade water was included as a negative control, and a known strain of *P. aeruginosa* (PAO1) used as a positive control. Following amplification, samples were examined by electrophoresis in 1 % agarose gels in 1× TBE buffer. Amplicons were purified using PureLink™ PCR Purification Kit (Invitrogen), and sequenced at the UC Berkeley DNA Sequencing Facility. Sequences were identified with BLAST (https://blast.ncbi.nlm.nih.gov).

2.7 Fluorescence *in situ* hybridization

Contact lenses removed from the mouse eye, cut in half with a sterile scalpel, and fixed in paraformaldehyde (2 %) for 1 h with shaking at RT. Bacterial hybridization was performed using a universal 16S rRNA gene probe [Alexa488]-GCTGCCTCCCGTAGGAGT-[Alexa488] (Eurofins Genomics) as previously described [46,47]. Briefly, fixed lenses and eyes were washed in 80% EtOH, 95% EtOH, and then PBS for 10 min each with shaking at RT. Lenses and eyes were then placed in a hybridization buffer solution [NaCl (0.9 M), Tris-HCl (20 mM, pH 7.2) and SDS (0.01 %)] and incubated at 55 °C for 30 min. The probe was added to a final concentration of 100 nM and incubated at 55 °C overnight. Lenses and eyes were then transferred to wash buffer solution [NaCl (0.9 M) and Tris-HCl (20 mM, pH 7.2)] and washed 3 times for 10 min each with shaking at RT. Lenses were mounted on slides and imaged using an Olympus FV1000 confocal microscope. A 488 nm laser was used for the detection of bacteria labeled by FISH, and a 635 nm laser was used to obtain contact lens reflections (excitation and emission at the same wavelength). Three or more random fields per sample were imaged in 0.5 μm steps, and 3D images were reconstructed from z-stacks using IMARIS software (Bitplane).

2.8 Statistical analysis

Quantitative data were expressed as a mean ± standard deviation or median with upper and lower quartiles. The Student's t-test was used to compare two groups. The Kruskal-Wallis

test or two-way ANOVA with Sidak's multiple comparison test were used to compare three or more groups. Survival curves were analyzed using Log-rank Mantel-Cox test. Prism was used for linear regression analysis, curve fitting, and the above statistical tests. P values < 0.05 were considered significant.

3. Results

3.1 Biomicroscopic and OCT evaluation of the murine contact lens and lens-wearing eye *in vivo*

A dissecting microscope was used to evaluate the parameters surrounding fit of the contact lens on the murine eye. After placement on the eye (mice aged 5–12 weeks) (see Supplemental Video S1), the lenses were found to cover most of the cornea with the lens periphery in close proximity to the limbus *in vivo* and *ex vivo* (Fig. 1a). Ocular Coherence Tomography (OCT) imaging of the lens *in-situ* showed a seamless fit over the corneal surface (Fig. 1b). After lens placement, mice were single-housed and fitted with an Elizabethan collar to prevent mice removing the lenses through grooming. Since reduced grooming caused dust and some discharge to build up on the conjunctiva, an alternate form of paper bedding was used that vastly improved ocular surface cleanliness. The contact lens retention rate *in vivo* was 63–73 % over 2 days, becoming 47 % after 7 days (Fig. 1c, left panel). Of the several factors investigated, only body weight had a significant effect on lens retention (Fig. 1c, right panel). Smaller body weights of 19 g or less were associated with a 57 % retention rate after 7 days, compared to body weights over 19 g showing a 30 % retention rate over the same period ($p < 0.05$, Log-rank Mantel-Cox test).

After fitting, lens-wearing eyes were compared to non-lens wearing contralateral controls daily using a dissecting microscope over a period of 2 to 14 days of lens wear. Corneas appeared healthy without visible signs of inflammation, injury, or opacity as compared to contralateral control eyes (Fig. 2). Worn lenses appeared relatively clear and remained hydrated as shown by their reflective wet front surface (Fig. 2, lower row), which was confirmed after removal.

3.2 Use of a membrane reporter mouse reveals multiple changes to corneal morphology during lens wear

To obtain more detail about the impact of lens wear, we used mice expressing membrane-localized td-tomato to compare lens wearing corneas to contralateral non-lens wearing corneas by high-resolution confocal microscopy. To account for the possibility that there might be effects on the contralateral eye induced by lens wear, or by Elizabethan collar use, we also included mice that were not fitted with lenses, with and without the use of collars, in the study. Corneas of contralateral control eyes of lens-wearing mice showed typical morphology, i.e., an intact multilayered epithelium above a stroma containing healthy interconnected keratocytes (Fig. 3a). These corneas were indistinguishable from those of non-lens-wearing mice with or without the Elizabethan collar (data not shown). However, significant alterations in the corneal epithelium and stroma were observed for lens-wearing eyes compared to contralateral controls. As seen in Fig. 3 (and Supplemental Video S2), after 14 days of continuous lens wear, small round vesicles (~1 to 4 μm diameter) were

visible in the most external layers of the corneal epithelium and were not present in controls. In the stroma, keratocyte morphology was visibly altered, with cell edges appearing jagged compared to the smooth profile of the keratocytes in contralateral eye controls (Fig. 3a and Supplemental Video S2). Moreover, the stroma contained numerous small cells not normally present. These cells appeared to be actively motile, seen trafficking along and over the surfaces of the stromal keratocytes, altering their position between image collection time intervals while acquiring high-resolution confocal z-stacks (pseudo time-lapse Supplemental Video S2). Real time-lapse video microscopy used over 30 min confirmed the presence of numerous highly motile round cells throughout the stroma (Fig. 3b and Supplemental Video S3). These cells were found as early as 5 days after initiation of lens wear.

3.3 Murine contact lens wear is associated with neutrophil recruitment into the corneal stroma dependent on IL-1R and MyD88

To investigate if the infiltrating cells seen with lens wear were myeloid-derived, we employed the CRE recombinase expressed in LysMcre mice, and crossed them with mT/mG mice harboring a CRE cassette that mediates the switch in expression from td-tomato to GFP (see Methods) to obtain a murine strain expressing membrane-localized GFP in granulocytes, mature macrophages and partially in dendritic cells (CD11c-positive) [48], and td-tomato in all other cell types. After 7 days of lens wear, morphological observations and shape measurements (area [A], perimeter [P] and circularity [C]), in z-projections of Fig. 4a (and Supplemental Video S4), allowed 4 types of cells expressing GFP (i.e. myeloid-derived) to be distinguished in the contralateral non-lens-wearing eyes. Based upon their appearance, cells were assigned to one of the following created categories: small round cells (#1, resembling neutrophils, A = 234 μm^2, P = 63 μm, Circ. = 0.740), large lobulated (#2, resembling macrophages, A = 861 μm^2, P = 195 μm, Circ. = 0.283), thin dendriform (#3, resembling dendritic cells, A = 390 μm^2, P = 358 μm, Circ. = 0.038) and extremely elongated (#4, resembling oligodendrocytes, A = 2294 μm^2, P = 804 μm, Circ. = 0.045). After 7 days of lens wear, a clear increase in the total number of cells was apparent in lens-fitted eyes (Fig. 4a, 4c [left panel], and Supplemental Video S4) that was absent in contralateral controls and naïve eyes (Fig. 4c, left panel). Indeed, both controls showed similar Lyz2-positive cell numbers indicating that lens-induced effects were specific to the fitted eyes. Morphological analysis (Fig. 4b and 4c [middle and right panels]) revealed a shift in cell shape after lens wear, indicated by an increase in area and decrease in perimeter (Fig. 4c, middle panel). Additionally, we measured an increase in the frequency of cells with higher circularity (Fig. 4b and 4c [right panel]). Fast-moving cells appeared to belong to the small round cell category (#1) as evident in time-lapse in Fig. 4d and Supplemental Videos S4 and S5.

The appearance and motility of these additional cells in the corneal stroma of lens-wearing eyes suggested infiltration of neutrophils, which are not usually present in the cornea. To test that hypothesis, we performed immunofluorescence imaging of corneal cryo-sections using antibodies against Ly6G, a neutrophil marker. The results confirmed the presence of a significant number of Ly6G-positive cells (suggesting neutrophils) that were not detected in contralateral control eyes (Fig. 5a). Quantification of Ly6G-positive cells after 6 days (Fig. 5c, left panel) confirmed these observations, while time-course studies indicated that Ly6G-

positive cell recruitment required a minimum of 5 days of continuous lens-wear (Fig. 5c, right panel), and it was maintained at a similar level for up to 14 days thereafter (data not shown).

To gain insights into the mechanisms for Ly6G-positive cell recruitment, and to begin to understand its significance, we also fitted MyD88 (−/−) and IL-1R (−/−) mice with lenses. The Ly6G-positive cell response to contact lens wear was found lacking in the corneas of these mice (Fig. 5b). Ly6G-positive cells were found in the limbal and conjunctival regions of wild-type, MyD88 (−/−) and IL-1R (−/−) mice with and without lens-wear for 6 days (Supplemental Fig. S1) with no significant difference between control and lens-wearing eyes in any group. While limbal and conjunctival regions of IL-1R (−/−) eyes showed a reduction in Ly6G-positive cells versus wild-type controls, the reduction was similar for control and lens-wearing eyes IL-1R (−/−) eyes, and was not observed in eyes of MyD88 (−/−) mice. Thus, these data suggest that the lack of Ly6G-positive cell recruitment into the corneas of lens-wearing MyD88 (−/−) or IL-1R (−/−) mice after 6 days (Fig. 5) involves defective recruitment from the limbus/conjunctiva.

The immunohistological images also allowed for examination of the impact of lens wear on corneal structure. They showed that the corneal epithelium and the remainder of the cornea remained intact despite the Ly6G-positive (neutrophil) response.

3.4 Lens wear altered CD11c-positive cell distribution in the central cornea

In human subjects, it has been shown that contact lens wear can alter the distribution of dendritic cells within the cornea even after only a few hours of wear [37–39]. Dendritic cells, which can be distinguished by their expression of CD11c, are known to be sentinel cells in mucosae and epithelia [49–51]. Indeed, we previously showed that CD11c-positive cells play important roles in early recognition of, and response to, *P. aeruginosa* at the ocular surface at 4 h [43]. Thus, we investigated CD11c-positive cell responses to contact lens wear using mice expressing YFP under control of the CD11c promoter. Contact lens wear was found to recruit CD11c-positive (dendritic) cells to the central cornea by 24 h (Fig. 6a, 6c [left panel]) with no further increase at later time points up to 6 days (Fig. 6a). As above (Fig. 4c, left panel), contralateral controls and naïve eyes showed no change in CD11c-positive cell numbers, and were similar to each other (Fig. 6c, left panel). Some CD11c-positive cells were found at the basal lamina with processes in the stroma and extending into the epithelium (Fig. 6b). However, the bimodal distribution of CD11c-positive cells within the central cornea was altered in lens-wearing mice after 24 h with their localization closer to the epithelial surface and the posterior corneal endothelium than in contralateral control eyes (Fig. 6c, center panel). An increase in corneal thickness was also observed in lens-wearing eyes after 24 h that was statistically significant (Fig. 6c, right panel). Increased thickness involved changes to both the stroma (control 62.2 +/− 1.8 μm versus lenswear 71.8 +/− 5.0 μm) and the epithelium (control 40.4 +/− 1.6 μm versus lens-wear 44.1 +/− 2.3 μm). However, each of these individual increases in thickness was not statistically significant.

3.5 Worn mouse contact lenses harbor commensal-type microbes

Previous studies in our laboratory showed that the healthy murine cornea contrasts with the adjacent conjunctiva in that it does not harbor a viable bacterial microbiome, a phenomenon dependent on IL-1R [40]. Even when extremely large quantities of bacteria (either pathogenic or commensals) are inoculated onto healthy non-lens wearing mouse eyes, the cornea uses IL-1R dependent strategies to clear them within 24 h [40]. Nevertheless, studies have shown that during human lens wear, the contact lens is often contaminated with microbes that are commensals of the adjacent conjunctiva and skin [41]. Here, we explored if worn mouse lenses also harbor microbes.

Lenses were removed from mice after 1 to 11 days of wear using sterile forceps, and lens homogenates examined for viable bacteria using standard techniques (see methods). The results revealed that culturable bacteria were present on 13 of 14 lenses, with *Corynebacterium* spp. being the most commonly identified (Table 1). Given that not all bacteria can be cultured, we also used FISH with a universal 16S rRNA gene probe on a subset of worn lenses to visualize bacteria. FISH demonstrated the presence of bacteria on both anterior and posterior sides of worn lenses with significantly more bacteria detected on posterior versus anterior surfaces, the latter showing no colonization for several lenses (Fig. 7a and 7b). Colonization was observed on each day of lens wear, with a small increase in bacterial numbers observed over the first 3 days, although this increase was not statistically significant (Fig. 7b).

A subgroup of 5 mice that had worn a lens for at least 5 days were studied for Ly6G-positive cell infiltration in addition to the identity and quantity of lens-colonizing bacteria using culture methods. As expected, Ly6G-positive cell infiltration was seen in lens-wearing corneas of all 5 mice. Of the 5 lenses removed from these eyes, 4 harbored *Corynebacterium* spp. as the predominant lens-colonizing bacteria, but no bacteria were recovered from the remaining lens (Table 1).

The FISH method was also used to determine if bacteria were also present on the surface of lens-wearing corneas. Very few bacteria were detected on corneas of either contact lens wearing or contralateral controls (Fig. 7c and 7d). On rare occasion, individual bacteria were detected within the corneal epithelium of contact lens-wearing eyes (example in Fig. 7d). Importantly, the presence of commensal bacteria (including a *Pseudomonas* sp. in one instance) on mouse contact lenses after wear (Table 1) did not result in development of microbial keratitis in any of the mice for up to 14 days of wear (Fig. 8a and 8b).

3.6 Murine lenses predispose the cornea to infection when contaminated with *P. aeruginosa*

The opportunistic pathogen *P. aeruginosa* is the most common cause of contact lens-related infection. This bacterium does not infect the healthy mouse cornea in the absence of contact lens wear unless there is deep penetrating injury that compromises the basal lamina beneath the corneal epithelium [30,52]. Previous studies using other species have shown that lens wear enhances susceptibility to *P. aeruginosa* infection in people, rats and rabbits, but not guinea pigs [15,23–25].

To explore if lens wear enables infection in the C57BL/6 mice used in this study, we inoculated lenses with *P. aeruginosa*, then cultured the bacteria overnight to achieve a final concentration of ~10^5 CFU per lens prior to fitting (see Methods). Microbial keratitis occurred as early as 24 h post-fitting (9 % of mice, Fig. 8b). Incidence of microbial keratitis increased with duration of wear (32 % of mice after 6 days, and 55 % of subjects after 11 days) (Fig. 8b). Bacteria isolated from mice with microbial keratitis (from the cornea and contact lens) were confirmed as *P. aeruginosa* from the original inoculum.

Corneas with microbial keratitis typically showed a loss of stromal organization and disruption of the basal epithelium. The remainder of the epithelium above the stroma appeared to be roughly intact, with cell membranes still attached to one another, although individual cells appeared to have altered morphology with more irregularities. In some corneas, clusters of small, round, fast-moving cells resembling the neutrophils in the stroma were seen within the corneal epithelium. In the example shown in Fig. 8d (Supplemental Video S6) these appeared to be coming from the stroma corresponding to the presence of a small, localized, corneal opacity. *P. aeruginosa* was observed penetrating the epithelium which appeared roughly intact and multilayered, but with disorganized epithelial cell structure, sometimes without observable corneal opacity (Fig. 8c). Within the epithelium, some cells were found to contain bacterial aggregates/microcolonies (Fig. 8c, arrows).

However, not all eyes fitted with *P. aeruginosa*-inoculated contact lenses became infected. In some mice, *P. aeruginosa* inoculated with the contact lens was cleared at variable times, with the eye showing no residual bacteria or pathology (see Supplemental Fig. S2).

4. Discussion

Contact lens wear is a widely used and a successful form of vision correction, but it carries a risk of complications, the most serious being a vision-threatening microbial keratitis. Understanding and resolving the pathogenesis of contact lens-related microbial keratitis, and other lens-related complications, requires suitable animal models that allow the effects of lens wear on corneal homeostasis to be determined at a molecular, cellular and tissue level. This depth of research investigation needed to understand and solve these problems is currently not possible using human subjects for multiple obvious reasons related to safety, ethics, and intrasubject variability.

In this study, we report development of a novel murine model of contact lens wear, enabling the many reagents and technologies available for mouse research to be utilized. Using the model, we showed it can faithfully mimic various biological phenomena occurring in human lens wear, including colonization of the lens with conjunctival and skin associated commensals [41], a rapid dendritic cell response [37–39], and enhanced susceptibility to infection with *P. aeruginosa* [17,53]. Beyond what can be done using human subjects, we also demonstrated a Ly6G-positive cell (likely neutrophil) response in the stroma requiring IL-1R and MyD88 following 5 days of lens wear that does not disrupt the transparency of the cornea and confirmed that the earlier dendritic-shaped cell response involves CD11c-positive cells. Using a mouse with red fluorescent (tdTomato expressing) membranes, with and without deliberate inoculation with green (GFP-expressing) bacteria, we have also been

able to observe changes to corneal cell morphology caused by lens wear with and without *P. aeruginosa* infection. Additionally, we detected *P. aeruginosa* in the process of traversing the corneal epithelium (and in some cells forming biofilm) in clear healthy-looking corneas, which is likely to be an early step in pathogenesis of lens-related infection difficult to study using injury models.

Neutrophil infiltration into the cornea generally causes collateral damage [24,27,54]. However, the Ly6G-positive cell (neutrophil) response during mouse lens wear occurred without associated changes to corneal transparency suggesting an alternate neutrophil phenotype with reduced generation of reactive oxygen species. Recent studies have demonstrated the plasticity and heterogeneity of neutrophils in health and disease [55–58]. Indeed, neutrophils have been shown to be required for corneal wound healing in some instances [59,60]. Further, quiescent neutrophils were recently shown to infiltrate the lung in a murine model of sterile lung injury [61].

The changes to the cornea induced by uninoculated contact lens wear over a period of 5 days in our murine model aligns well with the definition of para-inflammation. As described by Medzhitov in 2008, para-inflammation is a tissue adaptive response intermediate between basal tissue homeostasis and classical inflammation mediated by resident macrophages [62]. While not previously described in the cornea, para-inflammation is known to occur in the aging retina and it relates to the pathogenesis of some retinal diseases [63,64]. It is also thought to play a role in diabetes, atherosclerosis, age-related neurodegenerative diseases, obesity, and some forms of cancer [65,66]. The intended purpose of para-inflammation is to restore normal function and homeostasis in response to changes in the environment, but it can also have a dark side in the face of excessive stress, when it can turn into outright inflammation. Aspects of the response to mouse contact lens wear that suggest a para-inflammatory response include the dendritic cell changes observed after 24 h that persist over time, and the later infiltration of Ly6G-positive cells (neutrophils) into the stroma without an impact on corneal transparency or the epithelial barrier.

Considering that continuous lens wear is known to increase the risk of contact lens complications in people, it was interesting that the Ly6G-positive cell response occurred only after several days of continuous wear in mice. Future studies will be required to determine the relationship between this response and the pathogenesis of these complications. Since most people wear lenses on a daily wear basis, it would also be important to ascertain if removal of the lens for part of the day, and/or regular lens replacement prevents this phenomenon from occurring over several days of lens wear.

The trigger for the para-inflammatory response during contact lens wear and its function is yet to be established. Microbial antigens are likely contributors, and small numbers of bacteria were found colonizing worn lenses in our study. While there was a lens from which we could not culture bacteria that had been in an eye undergoing the parainflammatory response, culture methods can fail to detect viable bacteria if they are in a non-culturable state, and they cannot detect microbial debris (antigens) which can still trigger immune responses. The bacteria that were detected included *Corynebacterium* spp. and coagulase-negative *Staphylococcus* spp, which are commonly identified as conjunctival and skin

commensals in humans [67], readily colonize contact lenses [41], and are each involved in protective ocular immune responses to *P. aeruginosa* in scarification-injury murine models of corneal infection [68,69]. As such, the function of the parainflammatory response may be to prevent microbes from colonizing the cornea. Indeed, we did not find bacteria colonizing the cornea despite their presence on the lens. The requirement of IL-1R for these parainflammatory responses could also indicate microbial triggers [43,70,71], but would not exclude other potential (non-microbial) factors associated with the lens or post-lens environment that could activate endogenous danger-associated molecular patterns, with IL-1α and/or IL-1β release, and similar cellular responses [61,72–74].

Multiple mechanisms contribute to keeping the healthy cornea free of microbes when a lens is not worn. Indeed, the cornea normally lacks a microbiome despite constant exposure to microbes from the environment and adjacent colonized tissue surfaces [40]. It even resists colonization by potential pathogens introduced in large numbers [75,76], with resistance requiring IL-1R and MyD88 [40,77] of both epithelial cells and resident CD11c-positive cells [43], with contributions made by surfactant protein D, epithelial tight junctions, and antimicrobial peptides [75,76,78,79]. Antimicrobial peptide expression by the corneal epithelium can be constitutive and upregulated [80]. In the present study, the lack of corneal colonization by the commensal-type bacteria contaminating lenses, suggests mechanisms normally preventing microbiome establishment were not compromised, or that compensatory mechanisms were employed during lens wear. Whether para-inflammation plays a role in this respect is to be determined.

High magnification *ex vivo* imaging of mice expressing red fluorescent membranes showed subtle changes to cell morphology in lens-wearing corneas not observed using a dissecting microscope or immunohistochemistry. They included numerous small vesicles in epithelial cells and keratocytes appeared jagged. An increase in corneal thickness was also observed after 24 h. The significance of these changes is unclear, since corneal transparency was maintained in these eyes. Maintenance of corneal transparency is a complex regulated process dependent on the fine structure and biochemistry of the stroma, and on normal function of cells within all three cellular layers. Our data suggest, therefore, that CD11c-positive cell and neutrophil responses to lens wear did not functionally disrupt physiological processes that maintain corneal transparency, and/or that compensation mechanisms were in effect. It is also difficult to ascertain if some of the tissue changes, e.g. epithelial vesicles, are typical of para-inflammation, as other body sites are less amenable to detailed high-resolution imaging.

When mouse contact lenses were contaminated with *P. aeruginosa* before placement on the eye, an aggressive infiltrative response was observed in the stroma. The large number of infiltrating cells, rounded morphology, style of motility, and the damage to surrounding stroma and the basal epithelium, suggested a classical activated phagocyte, with high levels of oxidative burst and microbicidal activity. This aligns with published findings using the scarification injury model of *P. aeruginosa* infection, with essential roles for such cells in clearing infecting bacteria, and promoting disease resolution, but with a significant cost in collateral damage [27,30,31,81–85]. Mechanism(s) for the apparent change in neutrophil phenotype after *P. aeruginosa* challenge *via* the lens include pattern recognition receptors

and possibly bacterial virulence factors, such as the type three secretion system of *P. aeruginosa* that is known to modulate neutrophil migration and function [31,84,86,87]. In this respect, whether underlying lens-induced para-inflammation actually contributed to development of infection when mouse lenses were contaminated with *P. aeruginosa* is another open question. Alternatively, changes to ocular surface defense and microbial adaptations to the ocular surface [23] might drive disease initiation regardless of the presence or status of neutrophils in the cornea. Further work will be needed to delineate the respective roles of microbes and infiltrating cells in the pathogenesis of contact lens-related infection.

5. Conclusion

We have successfully developed a murine model of *in vivo* contact lens wear. The model faithfully replicates in mice several lens-associated phenomena previously reported in humans across a variety of lens materials, lenses from different manufacturers, different modalities of wear, and advances on what can be done using human subjects. Without the need to suture the eye shut to retain the lens, and its amenability to mouse-specific reagents, it also improves on existing larger animal models.

While the discovery that lens wear can cause a para-inflammatory response in mice is the first example of this type of response in the cornea, para-inflammation is known to be important in understanding health and disease at other body sites including the retina. This phenomenon might relate to multiple issues associated with contact lens wear, e.g. discomfort, inflammation and infection. For example, a recent study comparing reusable and daily disposable contact lens wear in humans revealed a positive association between lens discomfort and ratios of proinflammatory to anti-inflammatory tear cytokines, e.g. IL-1β to IL-10 [88]. Prior to that study, a perspective review of contact lens research in human subjects concluded that contact lens wear is “intrinsically inflammatory”, and suggested that para-inflammatory events were a part of uncomplicated lens wear, and might have a protective role [89]. Moreover, our data showing that *P. aeruginosa* can penetrate into the corneal epithelium during contact lens wear without injury provides important information about the role of lens wear in susceptibility to infection and is a phenomenon that cannot be demonstrated or properly studied using other mouse infection models.

With the projected escalation of contact lens use due to the need for myopia correction in humans, and contact lens use as an electronic device (e.g. for health monitoring), the development and availability of this novel murine model is timely. In addition to deciphering the mechanisms and relationships between phenomena occurring during lens wear and their significance, this model could also be of value to study impact of various contact lens-wearing modalities worn by people, e.g. differences between continuous wear as used in the present study, and daily removal with or without lens replacement. Beyond contact lens wear, this model provides another tool for researchers studying intrinsic mechanisms by which the cornea maintains health and transparency critical for vision and/or how it resists microbial colonization and infection.

Contrasting with other body sites, the cornea is ideal for imaging due to its transparency and superficial location. The response to contact lens wear in mice involves recruitment and morphological changes to multiple cell types while the cornea remains clear and amenable to high resolution intravital imaging using a standard confocal microscope. Thus, this model could also be useful for researchers outside the field of cornea research studying cellular, molecular and immunological processes in general or as they relate to other body sites.

Supplementary Material

Refer to Web version on PubMed Central for supplementary material.

Acknowledgements

Our thanks to Lisa Telford, Zena Gough, and Lee Norris (each from CooperVision Inc.) for their skillful assistance in murine lens fabrication.

Funding and disclosures

This work was supported by the National Institutes of Health EY024060 (SMJF). The funding source was not involved in study design, data collection or analysis, decision to publish or article preparation. Authors RF, LW, and MG are paid employees of CooperVision Inc. JM, TT, and CM were former paid employees of CooperVision Inc. CM is a consultant for CooperVision Inc. JM is presently a paid employee of Johnson and Johnson Inc.

References

[1]. Cope JR, Collier SA, Rao MM, Chalmers R, Mitchell LG, Richdale K, et al. Contact lens health week - Contact lens wearer demographics and risk behaviors for contact lensrelated eye infections - United States 2014. MMWR Morb Mortal Wkly Rep 2015;64:865–89. [PubMed: 26292204]

[2]. Stapleton F, Keay L, Jalbert I, Cole N. The epidemiology of contact lens related infiltrates. Optom Vis Sci 2007;84:257–72. [PubMed: 17435509]

[3]. Nichols JJ, Willcox MDP, Bron AJ, Belmonte C, Ciolino JB, Craig JP, et al. The TFOS international workshop on contact lens discomfort: Executive summary. Investig Ophthalmol Vis Sci 2013;54.

[4]. Wu PC, Huang HM, Yu HJ, Fang PC, Chen CT. Epidemiology of myopia. Asia-Pacific J Ophthalmol 2016;5:386–93.

[5]. ElShaer A, Ghatora B, Mustafa S, Alany RG. Contact lenses as drug reservoirs & delivery systems: the successes & challenges. Ther Deliv 2014;5:1085–100. [PubMed: 25418268]

[6]. Ciolino JB, Stefanescu CF, Ross AE, Salvador-Culla B, Cortez P, Ford EM, et al. In vivo performance of a drug-eluting contact lens to treat glaucoma for a month. Biomaterials 2014;35:432–9. [PubMed: 24094935]

[7]. Phan CM, Subbaraman L, Jones LW. The use of contact lenses as biosensors. Optom Vis Sci 2016;93:419–25. [PubMed: 26657694]

[8]. Farandos NM, Yetisen AK, Monteiro MJ, Lowe CR, Yun SH. Contact lens sensors in ocular diagnostics. Adv Healthc Mater 2015;4:792–810. [PubMed: 25400274]

[9]. Park J, Kim J, Kim S-Y, Cheong WH, Jang J, Park Y-G, et al. Soft, smart contact lenses with integrations of wireless circuits, glucose sensors, and displays. Sci Adv 2018;4:eaap9841. [PubMed: 29387797]

[10]. Willcox MD, Holden BA. Contact lens related corneal infections. Biosci Rep 2001;21:445–61. [PubMed: 11900321]

[11]. Stapleton F, Carnt N. Contact lens-related microbial keratitis: how have epidemiology and genetics helped us with pathogenesis and prophylaxis. Eye 2012;26:185–93. [PubMed: 22134592]

[12]. Wu YTY, Willcox M, Zhu H, Stapleton F. Contact lens hygiene compliance and lens case contamination: A review. Contact Lens Anterior Eye 2015;38:307–16. [PubMed: 25980811]

[13]. Lim CHL, Carnt NA, Farook M, Lam J, Tan DT, Mehta JS, et al. Risk factors for contact lens-related microbial keratitis in Singapore. Eye 2016;30:447–55. [PubMed: 26634710]

[14]. Schein OD, Buehler PO, Stamler JF, Verdier DD, Katz J. The impact of overnight wear on the risk of contact lens-associated ulcerative keratitis. Arch Ophthalmol 1994;112:186–90. [PubMed: 8311770]

[15]. Stapleton F, Keay L, Edwards K, Naduvilath T, Dart JKG, Brian G, et al. The Incidence of contact lens-related microbial keratitis in Australia. Ophthalmology 2008;115:1655–62. [PubMed: 18538404]

[16]. Sorbara L, Jones L, Williams-Lyn D. Contact lens induced papillary conjunctivitis with silicone hydrogel lenses. Cont Lens Anterior Eye 2009;32:93–6. [PubMed: 19181562]

[17]. Stapleton F, Keay L, Edwards K, Holden B. The epidemiology of microbial keratitis with silicone hydrogel contact lenses. Eye Contact Lens 2013;39:79–85. [PubMed: 23172318]

[18]. Chalmers RL, Keay L, McNally J, Kern J. Multicenter case-control study of the role of lens materials and care products on the development of corneal infiltrates. Optom Vis Sci 2012;89:316–25. [PubMed: 22227912]

[19]. Dumbleton K, Woods CA, Jones LW, Fonn D. The impact of contemporary contact lenses on contact lens discontinuation. Eye Contact Lens Sci Clin Pract 2013;39:92–8.

[20]. Robertson DM, Cavanagh HD. Non-compliance with contact lens wear and care practices: a comparative analysis. Optom Vis Sci 2011;88:1402–8. [PubMed: 21946785]

[21]. Szliter EA, Morris CA, Carney F, Gabriel MM, Hazlett LD. Development of a new extended-wear contact lens model in the rat. CLAO J 2002;28:119–23. [PubMed: 12144229]

[22]. Zhang Y, Gabriel MM, Mowrey-McKee MF, Barrett RP, McClellan S, Hazlett LD. Rat silicone hydrogel contact lens model: effects of high-versus low-Dk lens wear. Eye Contact Lens 2008;34:306–11. [PubMed: 18997538]

[23]. Tam C, Mun JJ, Evans DJ, Fleiszig SM. The impact of inoculation parameters on the pathogenesis of contact lens-related infectious keratitis. Invest Ophthalmol Vis Sci 2010;51:3100–6. [PubMed: 20130275]

[24]. Wei C, Zhu M, Matthew Petroll W, Robertson DM. Pseudomonas aeruginosa infectious keratitis in a high oxygen transmissible rigid contact lens rabbit model. Investig Ophthalmol Vis Sci 2014;55:5890–9. [PubMed: 25125601]

[25]. Vijay AK, Sankaridurg P, Zhu H, Willcox MDP. Guinea pig models of acute keratitis responses. Cornea 2009;28:1153–9. [PubMed: 19770709]

[26]. Lawin-Brussel CA, Refojo MF, Leong FL, Hanninen L, Kenyon KR. Effect of *Pseudomonas aeruginosa* concentration in experimental contact lens-related microbial keratitis. Cornea 1993;12:10–8. [PubMed: 8458227]

[27]. Hazlett LD. Corneal response to Pseudomonas aeruginosa infection. Prog Retin Eye Res 2004;23:1–30. [PubMed: 14766315]

[28]. Hazlett LD, Hendricks RL. Reviews for immune privilege in the year 2010: immune privilege and infection. Ocul Immunol Inflamm 2010;18:237–43. [PubMed: 20662654]

[29]. Willcox MDP. *Pseudomonas aeruginosa* infection and inflammation during contact lens wear: a review. Optom Vis Sci 2007;84:273–8. [PubMed: 17435510]

[30]. Lee EJ, Cowell BA, Evans DJ, Fleiszig SM. Contribution of ExsA-regulated factors to corneal infection by cytotoxic and invasive *Pseudomonas aeruginosa* in a murine scarification model. Invest Ophthalmol Vis Sci 2003;44:3892–8. [PubMed: 12939306]

[31]. Zolfaghar I, Evans DJ, Ronaghi R, Fleiszig SMJ. Type III secretion-dependent modulation of innate immunity as one of multiple factors regulated by *Pseudomonas aeruginosa* RetS. Infect Immun 2006;74:3880–9. [PubMed: 16790760]

[32]. Choy MH, Stapleton F, Willcox MDP, Zhu H. Comparison of virulence factors in *Pseudomonas aeruginosa* strains isolated from contact lens- and non-contact lensrelated keratitis. J Med Microbiol 2008;57:1539–46. [PubMed: 19018027]

[33]. Evans DJ, Fleiszig SMJ. Why does the healthy cornea resist *Pseudomonas aeruginosa* infection? Am J Ophthalmol 2013;155:961–70. [PubMed: 23601656]

[34]. Sullivan AB, Tam KPC, Metruccio MME, Evans DJ, Fleiszig SMJ. The importance of the *Pseudomonas aeruginosa* type III secretion system in epithelium traversal depends upon conditions of host susceptibility. Infect Immun 2015;83:1629–40. [PubMed: 25667266]

[35]. Lin CC, Lalitha P, Srinivasan M, Prajna NV, McLeod SD, Acharya NR, et al. Seasonal trends of microbial keratitis in South India. Cornea 2012;31:1123–7. [PubMed: 22868629]

[36]. Somabhai Katara R, Dhanjibhai Patel N, Sinha M. A clinical microbiological study of corneal ulcer patients at western Gujarat, India. Acta Med Iran 2013;51:399–403. [PubMed: 23852845]

[37]. Alzahrani Y, Pritchard N, Efron N. Changes in corneal Langerhans cell density during the first few hours of contact lens wear. Contact Lens Anterior Eye 2016;39:307–10. [PubMed: 26923921]

[38]. Alzahrani Y, Colorado LH, Pritchard N, Efron N. Longitudinal changes in Langerhans cell density of the cornea and conjunctiva in contact lens-induced dry eye. Clin Exp Optom 2017;100:33–40. [PubMed: 27353750]

[39]. Sindt CW, Grout TK, Brice Critser D, Kern JR, Meadows DL. Dendritic immune cell densities in the central cornea associated with soft contact lens types and lens care solution types: A pilot study. Clin Ophthalmol 2012;6:511–9. [PubMed: 22536045]

[40]. Wan SJ, Sullivan AB, Shieh P, Metruccio MMEE, Evans DJ, Bertozzi CR et al. IL-1R and MyD88 contribute to the absence of a bacterial microbiome on the healthy murine cornea. Front Microbiol 2018;9:1117. [PubMed: 29896179]

[41]. Willcox MDP. Microbial adhesion to silicone hydrogel lenses: A review. Eye Contact Lens 2013;39:61–6. [PubMed: 23266589]

[42]. Jolly AL, Agarwal P, Metruccio MME, Spiciarich DR, Evans DJ, Bertozzi CR, et al. Corneal surface glycosylation is modulated by IL-1R and *Pseudomonas aeruginosa* challenge but is insufficient for inhibiting bacterial binding. FASEB J 2017;31:2393–404. [PubMed: 28223334]

[43]. Metruccio MME, Tam C, Evans DJ, Xie AL, Stern ME, Fleiszig SMJ. Contributions of MyD88-dependent receptors and CD11c-positive cells to corneal epithelial barrier function against Pseudomonas aeruginosa. Sci Rep 2017;7:13829. [PubMed: 29062042]

[44]. Bloemberg GV, O'Toole G a, Lugtenberg BJ, Kolter R. Green fluorescent protein as a marker for *Pseudomonas* spp. Appl Environ Microbiol 1997;63:4543–51. [PubMed: 9361441]

[45]. James G Universal bacterial identification by PCR and DNA sequencing of 16S rRNA gene In: Schuller M, Sloots PT, James SG, Halliday LC and Carter WJI, Eds., PCR for Clinical Microbiology, Springer, Dordrecht, 2010:209–14.

[46]. Mark Welch JL, Rossetti BJ, Rieken CW, Dewhirst FE, Borisy GG. Biogeography of a human oral microbiome at the micron scale. Proc Natl Acad Sci U S A 2016;113:E791800.

[47]. Vaishnava S, Yamamoto M, Severson KM, Ruhn KA, Yu X, Koren O, et al. The antibacterial lectin RegIIIγ promotes the spatial segregation of microbiota and host in the intestine. Science 2011;334:255–8. [PubMed: 21998396]

[48]. Clausen BE, Burkhardt C, Reith W, Renkawitz R, Förster I. Conditional gene targeting in macrophages and granulocytes using LysMcre mice. Transgenic Res 1999;8:265–77. [PubMed: 10621974]

[49]. Zoltán Veres T, Voedisch S, Spies E, Tschernig T, Braun A. Spatiotemporal and functional behavior of airway dendritic cells visualized by two-photon microscopy. Am J Pathol 2011;179:603–9. [PubMed: 21708113]

[50]. Arques JL, Hautefort I, Ivory K, Bertelli E, Regoli M, Clare S, et al. Salmonella induces flagellin- and MyD88-dependent migration of bacteria-capturing dendritic cells into the gut lumen. Gastroenterology 2009;137:579–587. [PubMed: 19375423]

[51]. Seyed-Razavi Y, Hickey MJ, Kuffová L, McMenamin PG, Chinnery HR. Membrane nanotubes in myeloid cells in the adult mouse cornea represent a novel mode of immune cell interaction. Immunol Cell Biol 2013;91:89–95. [PubMed: 23146944]

[52]. Hazlett LD, Berk RS. Effect of C3 depletion on experimental *Pseudomonas aeruginosa* ocular infection: histopathological analysis. Infect Immun 1984;43:783–90. [PubMed: 6698607]

[53]. Green M, Apel A, Stapleton F. A longitudinal study of trends in keratitis in Australia. Cornea 2008;27:33–9. [PubMed: 18245964]

[54]. Pearlman E, Sun Y, Roy S, Karmakar M, Hise AG, Szczotka-Flynn L, et al. Host defense at the ocular surface. Int Rev Immunol 2013;32:4–18. [PubMed: 23360155]

[55]. Bird L Immune regulation: Controlling neutrophil plasticity. Nat Rev Immunol 2010;10:752.

[56]. Kolaczkowska E, Kubes P. Neutrophil recruitment and function in health and inflammation. Nat Rev Immunol 2013;13:159–75. [PubMed: 23435331]

[57]. Tsuda Y, Takahashi H, Kobayashi M, Hanafusa T, Herndon DN, Suzuki F. Three different neutrophil subsets exhibited in mice with different susceptibilities to infection by methicillin-resistant *Staphylococcus aureus*. Immunity 2004;21:215–26. [PubMed: 15308102]

[58]. Deniset JF, Kubes P. Neutrophil heterogeneity: Bona fide subsets or polarization states? J Leukoc Biol 2018;103:829–38. [PubMed: 29462505]

[59]. Gan L, Fagerholm P, Kim HJ. Effect of leukocytes on corneal cellular proliferation and wound healing. Invest Ophthalmol Vis Sci 1999;40:575–81. [PubMed: 10067960]

[60]. Li Z, Burns AR, Smith CW. Two waves of neutrophil emigration in response to corneal epithelial abrasion: Distinct adhesion molecule requirements. Investig Opthalmology Vis Sci 2006;47:1947–55.

[61]. Tian X, Sun H, Casbon A-JJ, Lim E, Francis KP, Hellman J, et al. NLRP3 inflammasome mediates dormant neutrophil recruitment following sterile lung injury and protects against subsequent bacterial pneumonia in mice. Front Immunol 2017;8:1337. [PubMed: 29163464]

[62]. Medzhitov R. Origin and physiological roles of inflammation. Nature 2008;454:428–35. [PubMed: 18650913]

[63]. Chen M, Xu H. Parainflammation, chronic inflammation, and age-related macular degeneration. J Leukoc Biol 2015;98:713–25. [PubMed: 26292978]

[64]. Xu H, Chen M, Forrester JV. Para-inflammation in the aging retina. Prog Retin Eye Res 2009;28:348–68. [PubMed: 19560552]

[65]. Rea IM, Gibson DS, McGilligan V, McNerlan SE, Alexander HD, Ross OA. Age and agerelated diseases: Role of inflammation triggers and cytokines. Front Immunol 2018;9:586. [PubMed: 29686666]

[66]. Aran D, Lasry A, Zinger A, Biton M, Pikarsky E, Hellman A, et al. Widespread parainflammation in human cancer. Genome Biol 2016;17:145. [PubMed: 27386949]

[67]. Willcox MDP. Characterization of the normal microbiota of the ocular surface. Exp Eye Res 2013;117:99–105. [PubMed: 23797046]

[68]. Kugadas A, Christiansen SH, Sankaranarayanan S, Surana NK, Gauguet S, Kunz R, et al. Impact of microbiota on resistance to ocular Pseudomonas aeruginosa-induced keratitis. PLOS Pathog 2016;12:e1005855. [PubMed: 27658245]

[69]. St. Leger AJ, Desai JV, Drummond RA, Kugadas A, Almaghrabi F, Silver P, et al. An ocular commensal protects against corneal infection by driving an interleukin-17 response from mucosal γδ T cells. Immunity 2017;47:148–158. [PubMed: 28709803]

[70]. Altmeier S, Toska A, Sparber F, Teijeira A, Halin C, LeibundGut-Landmann S. IL-1 coordinates the neutrophil response to C. albicans in the oral mucosa. PLOS Pathog 2016;12:e1005882. [PubMed: 27632536]

[71]. Metruccio MME, Evans DJ, Gabriel MM, Kadurugamuwa JL, Fleiszig SMJ. Pseudomonas aeruginosa outer membrane vesicles triggered by human mucosal fluid and lysozyme can prime host tissue surfaces for bacterial adhesion. Front Microbiol 2016;7:1–19. [PubMed: 26834723]

[72]. Takenouchi T, Tsukimoto M, Hashimoto M, Kitani H. Inflammasome activation by danger signals: extracellular ATP and pH. Inflammasome 2014;1:8.

[73]. Gombault A, Baron L, Couillin I. ATP release and purinergic signaling in NLRP3 inflammasome activation. Front Immunol 2012;3:414. [PubMed: 23316199]

[74]. Rabolli V, Badissi AA, Devosse R, Uwambayinema F, Yakoub Y, Palmai-Pallag M, et al. The alarmin IL-1α is a master cytokine in acute lung inflammation induced by silica micro- and nanoparticles. Part Fibre Toxicol 2014;11:69. [PubMed: 25497724]

[75]. Mun JJ, Tam C, Kowbel D, Hawgood S, Barnett MJ, Evans DJ, et al. Clearance of *Pseudomonas aeruginosa* from a healthy ocular surface involves surfactant protein D and is compromised by bacterial elastase in a murine null-infection model. Infect Immun 2009;77:2392–8. [PubMed: 19349424]

[76]. Augustin DK, Heimer SR, Tam C, Li WY, Le Due JM, Evans DJ, et al. Role of defensins in corneal epithelial barrier function against *Pseudomonas aeruginosa* traversal. Infect Immun 2011;79:595–605. [PubMed: 21115716]

[77]. Tam C, LeDue J, Mun JJ, Herzmark P, Robey EA, Evans DJ, et al. 3D quantitative imaging of unprocessed live tissue reveals epithelial defense against bacterial adhesion and subsequent traversal requires MyD88. PLoS One 2011;6:e24008. [PubMed: 21901151]

[78]. Alarcon I, Tam C, Mun JJ, LeDue J, Evans DJ, Fleiszig SM. Factors impacting corneal epithelial barrier function against *Pseudomonas aeruginosa* traversal. Invest Ophthalmol Vis Sci 2011;52:1368–77. [PubMed: 21051692]

[79]. Tam C, Mun JJ, Evans DJ, Fleiszig SM. Cytokeratins mediate epithelial innate defense through their antimicrobial properties. J Clin Invest 2012;122:3665–77. [PubMed: 23006328]

[80]. McDermott AM, Redfern RL, Zhang B, Pei Y, Huang L, Proske RJ. Defensin expression by the cornea: multiple signalling pathways mediate IL-1beta stimulation of hBD-2 expression by human corneal epithelial cells. I*nvest Ophthalmol Vis Sci* 2003;44:1859–65. [PubMed: 12714616]

[81]. Hazlett LD, Zucker M, Berk RS. Distribution and kinetics of the inflammatory cell response to ocular challenge with *Pseudomonas aeruginosa* in susceptible versus resistant mice. Ophthalmic Res 1992;24:32–9.

[82]. Pearlman E, Johnson A, Adhikary G, Sun Y, Chinnery HR, Fox T, et al. Toll-like receptors at the ocular surface. Ocul Surf 2008;6:108–16. [PubMed: 18781257]

[83]. Wu M, Peng A, Sun M, Deng Q, Hazlett LD, Yuan J, et al. TREM-1 amplifies corneal inflammation after *Pseudomonas aeruginosa* infection by modulating Toll-like receptor signaling and Th1/Th2-type immune responses. Infect Immun 2011;79:2709–16. [PubMed: 21555403]

[84]. Sun Y, Karmakar M, Taylor PR, Rietsch A, Pearlman E. ExoS and ExoT ADP ribosyltransferase activities mediate *Pseudomonas aeruginosa* keratitis by promoting neutrophil apoptosis and bacterial survival. J Immunol 2012;188:1884–95. [PubMed: 22250085]

[85]. Tam C, Lewis SE, Li WY, Lee E, Evans DJ, Fleiszig SMJ. Mutation of the phospholipase catalytic domain of the *Pseudomonas aeruginosa* cytotoxin ExoU abolishes colonization promoting activity and reduces corneal disease severity. Exp Eye Res 2007;85:799–805. [PubMed: 17905228]

[86]. Vareechon C, Zmina SE, Karmakar M, Pearlman E, Rietsch A. Pseudomonas aeruginosa Effector ExoS Inhibits ROS Production in Human Neutrophils. Cell Host Microbe 2017;21:611–8. [PubMed: 28494242]

[87]. Garrity-Ryan L, Kazmierczak B, Kowal R, Comolli J, Hauser A, Engel JN. The arginine finger domain of ExoT contributes to actin cytoskeleton disruption and inhibition of internalization of *Pseudomonas aeruginosa* by epithelial cells and macrophages. Infect Immun 2000;68:7100–13. [PubMed: 11083836]

[88]. Chao C, Stapleton F, Willcox MDP, Golebiowski B, Richdale K. Preinflammatory signs in established reusable and disposable contact lens wearers. Optom Vis Sci 2017;94:1003–8. [PubMed: 28858005]

[89]. Efron N Contact lens wear is intrinsically inflammatory. Clin Exp Optom 2017;100:3–19. [PubMed: 27806431]

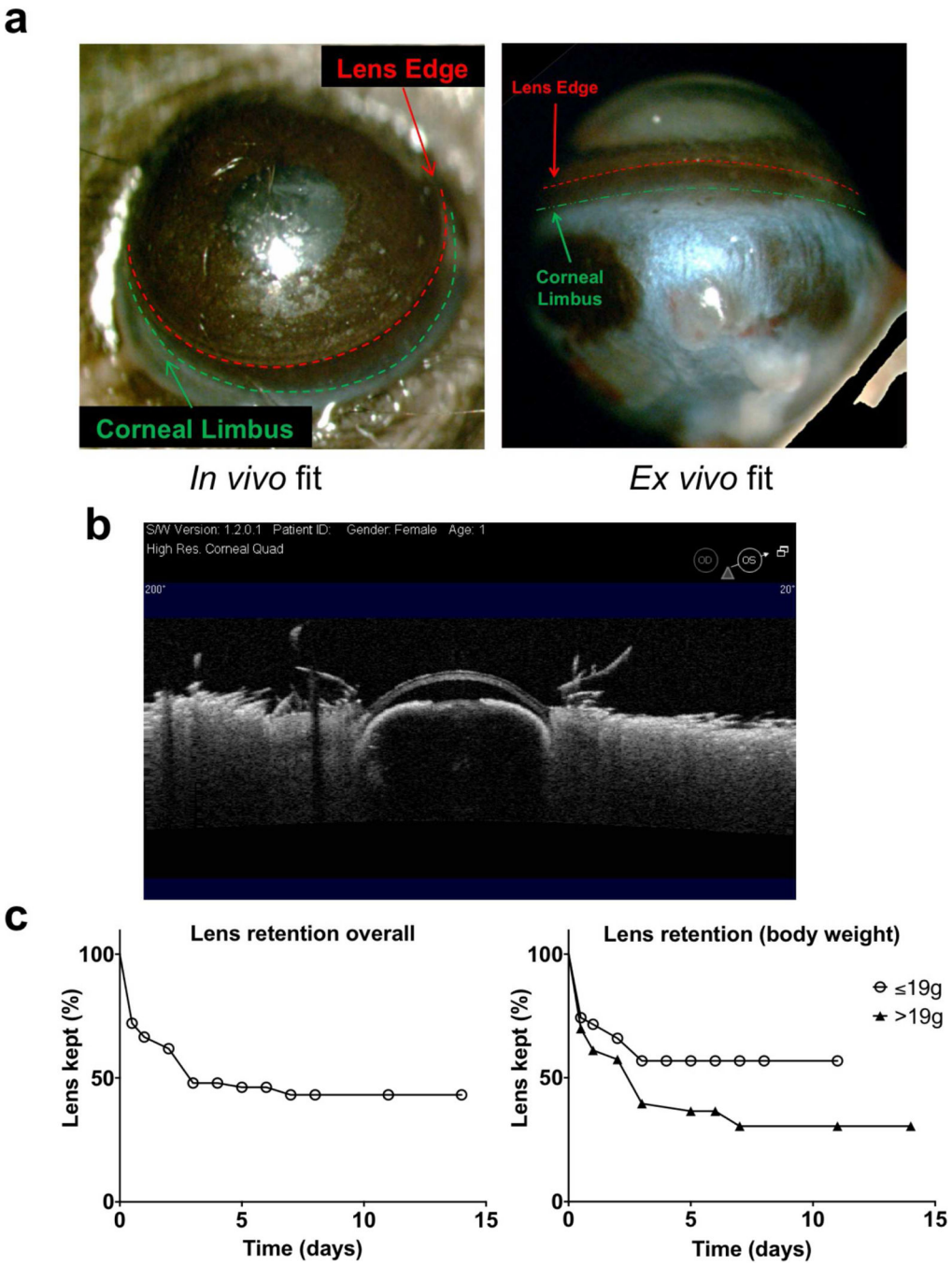

Fig. 1.

Fitting of custom-made contact lenses in 6 to 12 weeks old C57BL/6 mice. (a) Dissecting microscope images (acquired *in vivo* and *ex vivo*) showing the contact lens covering most of the murine cornea excluding the limbus and conjunctiva. (b) Optical coherence tomography (OCT) image showing close alignment of the contact lens to the murine cornea over its entire surface. (c) Overall contact lens retention rate (left panel, n° 147 subjects), and retention rates according to body weight (right panel, n° 74 ≤ 19 g and N° 73 > 19 g). Mice

with a body weight of ≤ 19 g showed a significantly different retention curve compared to those with a body weight of > 19 g ($p < 0.05$, Log-rank Mantel-Cox test).

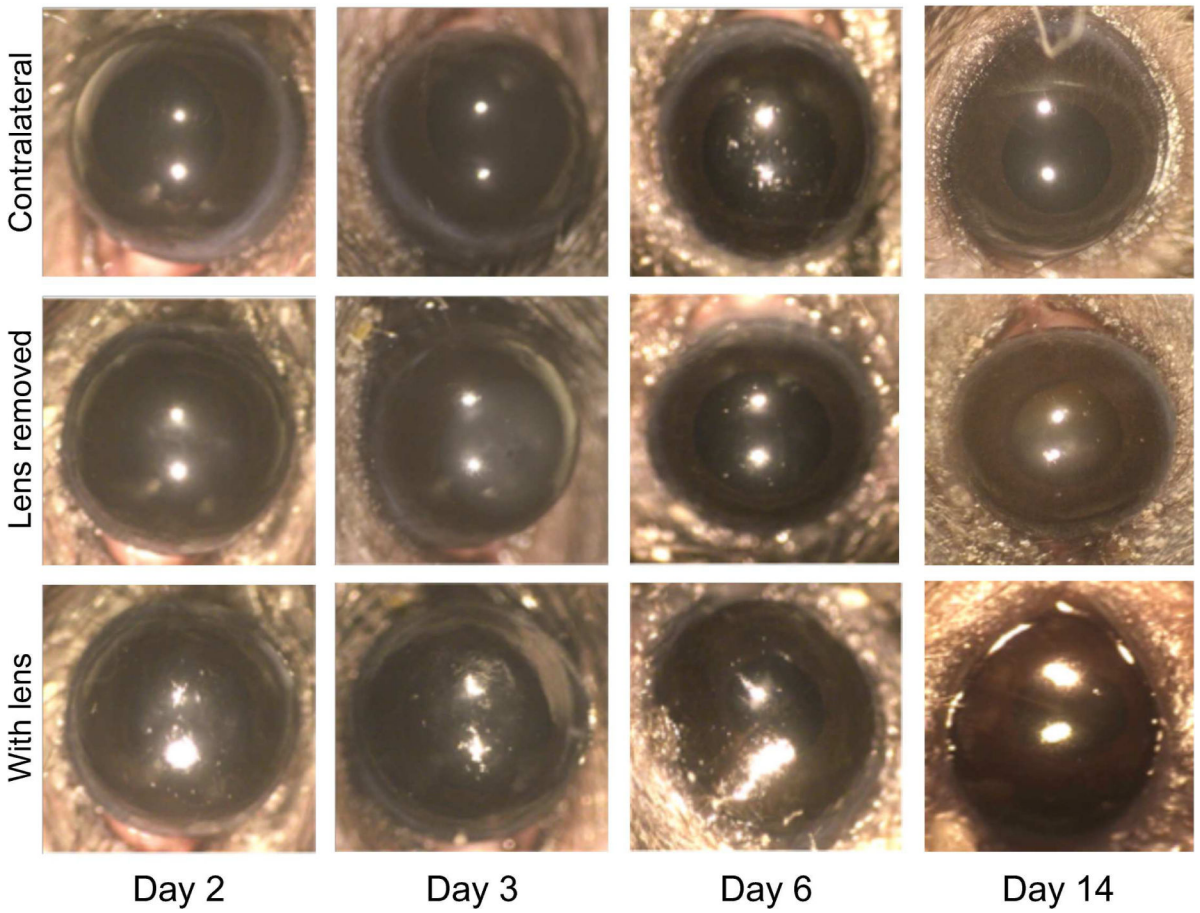

Fig. 2.

In vivo images of mouse eyes wearing a contact lens (bottom row), after removing the contact lens (central row) and contralateral controls (top row) were taken using a dissecting microscope at indicated time-points. Although some alteration in the reflective properties and smoothness of the contact lens could be observed in some cases, all corneas appeared healthy and transparent with no signs of opacity or scratches at all time-points, and only minimal debris accumulation on the contact lenses (bottom row).

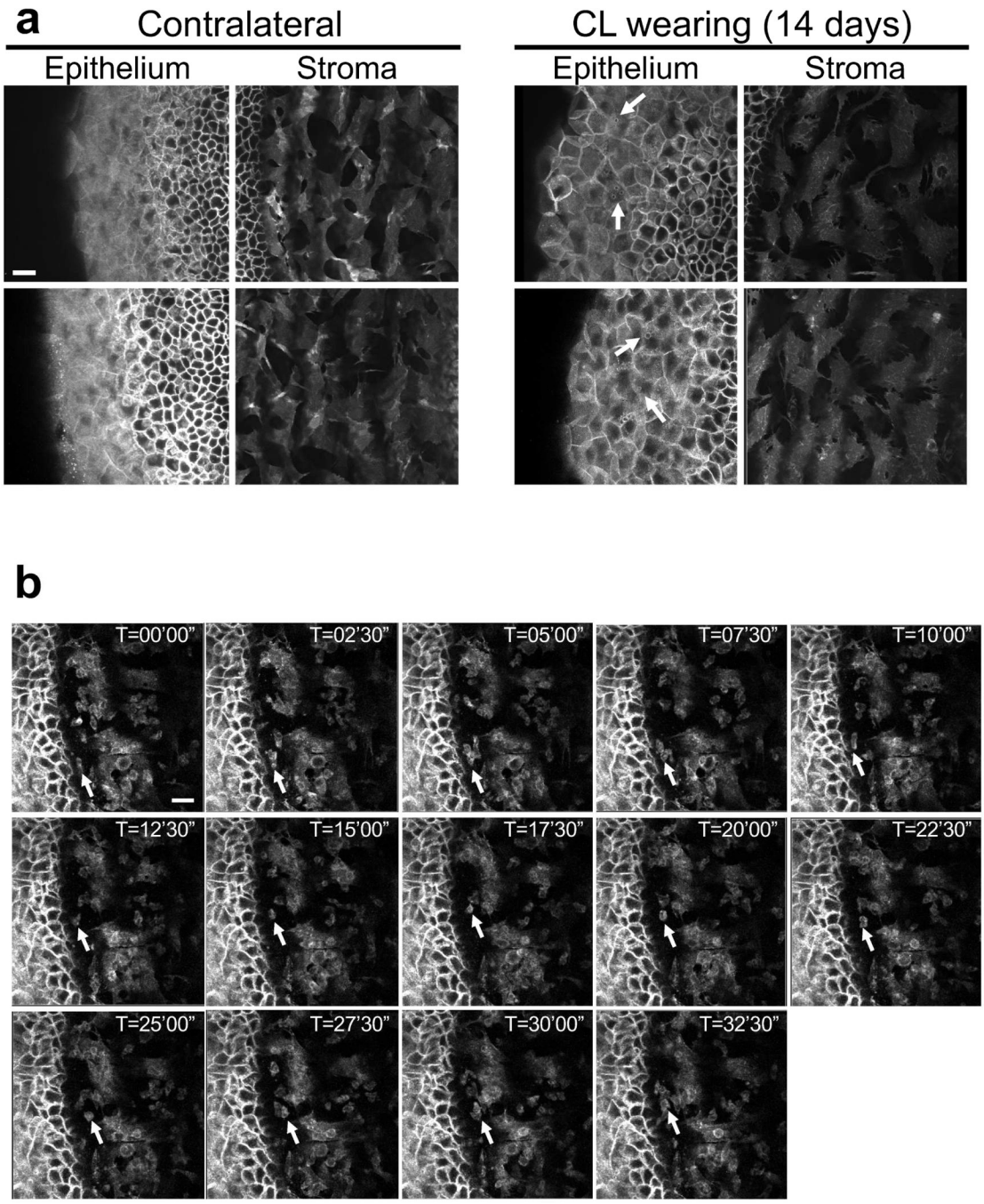

Fig. 3.

Confocal imaging of murine corneas after 14 days contact lens wear. Mice expressing td-tomato protein in all cell membranes were used. (a) Confocal optical sections showing the presence of multiple small vesicles (arrows) in the epithelium of lens-wearing corneas, absent in contralateral eyes. Stromal keratocytes of lens-wearing eyes showed altered morphology with most showing jagged cell edges compared to the smoother profile of keratocytes in control corneas. (b) Time-lapse images showing multiple small round cells

moving across the keratocytes in the stroma of contact lens wearing eyes (arrow shows one example) over a 32 min, 30 sec time-span. White bar = 20 μm.

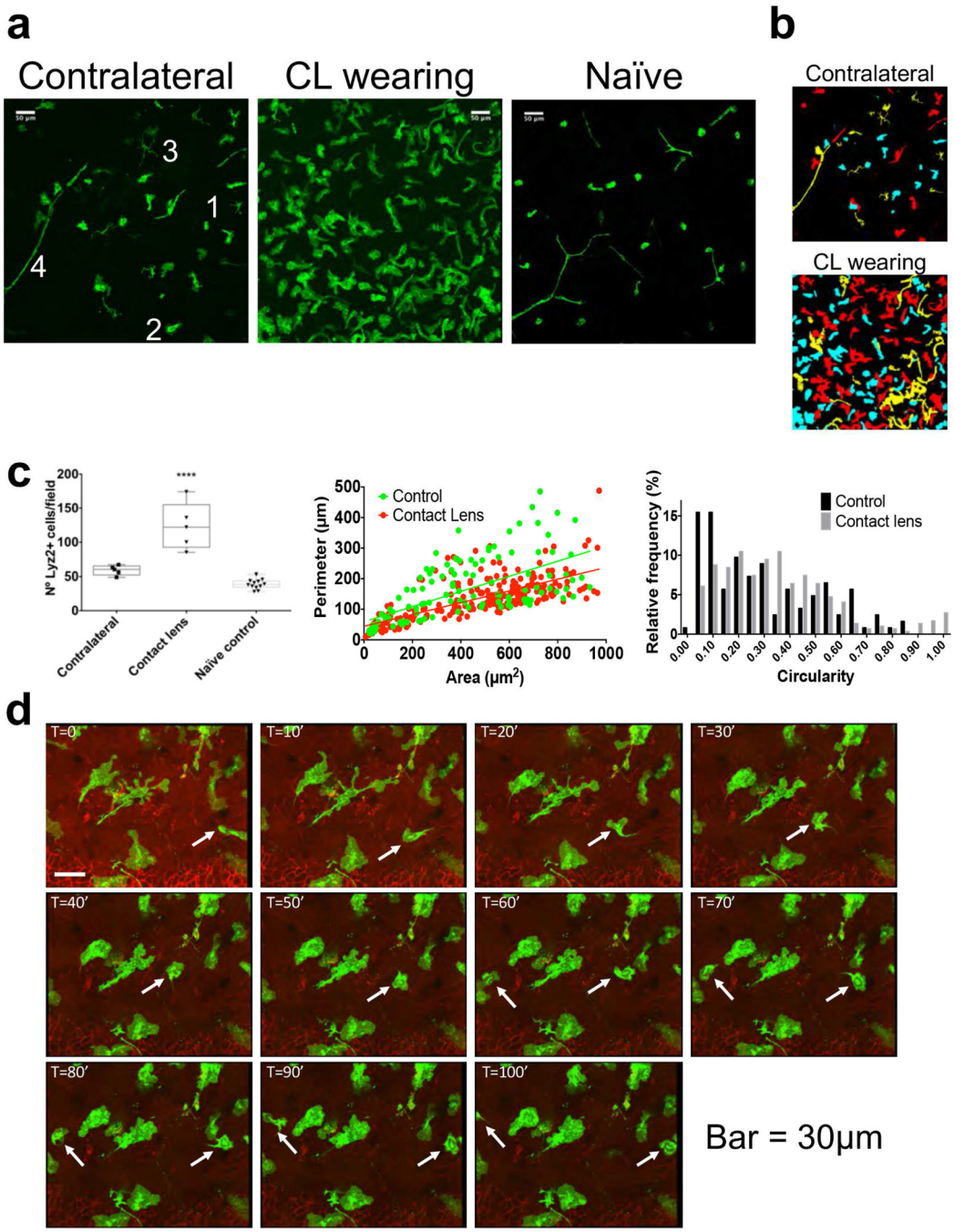

Fig. 4.

Multiple Lyz2$^+$ (myeloid-derived) cells respond to contact lens wear. (a) Z-projections of the GFP channel (all Lyz2$^+$ cells projected into one plane) in the central cornea of a mT/mGLysMcre hybrid mouse (see Methods) after 7 days of continuous lens wear compared to the contralateral control and a naïve eye. Numbers indicate the different myeloid-derived cell types observed based on morphology (see Results). Scale bar = 50 µm. (b) Same field as in (a) for contralateral control and lens-wearing eyes after Morpholib morphological segmentation (see Methods) and color-coding based on circularity arbitrarily divided in 3

groups, each accounting for a third of the total cell number (yellow ≤ 0.1, red 0.1 < > 0.3 and cyan ≥ 0.3. (c) Left panel shows quantification of Lyz2+ cells per field of view in contact lens-wearing corneas versus contralateral controls and naïve eyes (**** $p < 0.0001$, Kruskal-Wallis test). Middle and right panels show the quantification of morphological parameters of $Lyz2^+$ cells from contact lenswearing corneas versus contralateral controls. Image analysis was performed using MorpholibJ tools for 3D segmentation in ImageJ and parameters related to z-projections used (perimeter, area and circularity) to exclude artifacts due to lower z resolution. The middle panel shows the corneal distribution of individual cells based on area and perimeter with a linear regression fit indicating two significantly different curves ($p = 0.0325$). The right panel shows the relative frequency distribution based on $Lyz2^+$ cell circularity. (d) Time-lapse images showing multiple $Lyz2^+$ cells in the corneal stroma of a contact lens-wearing eye with two small round cells moving at considerable speed (arrows) over a 100 min time-span. White bar = 20 μm.

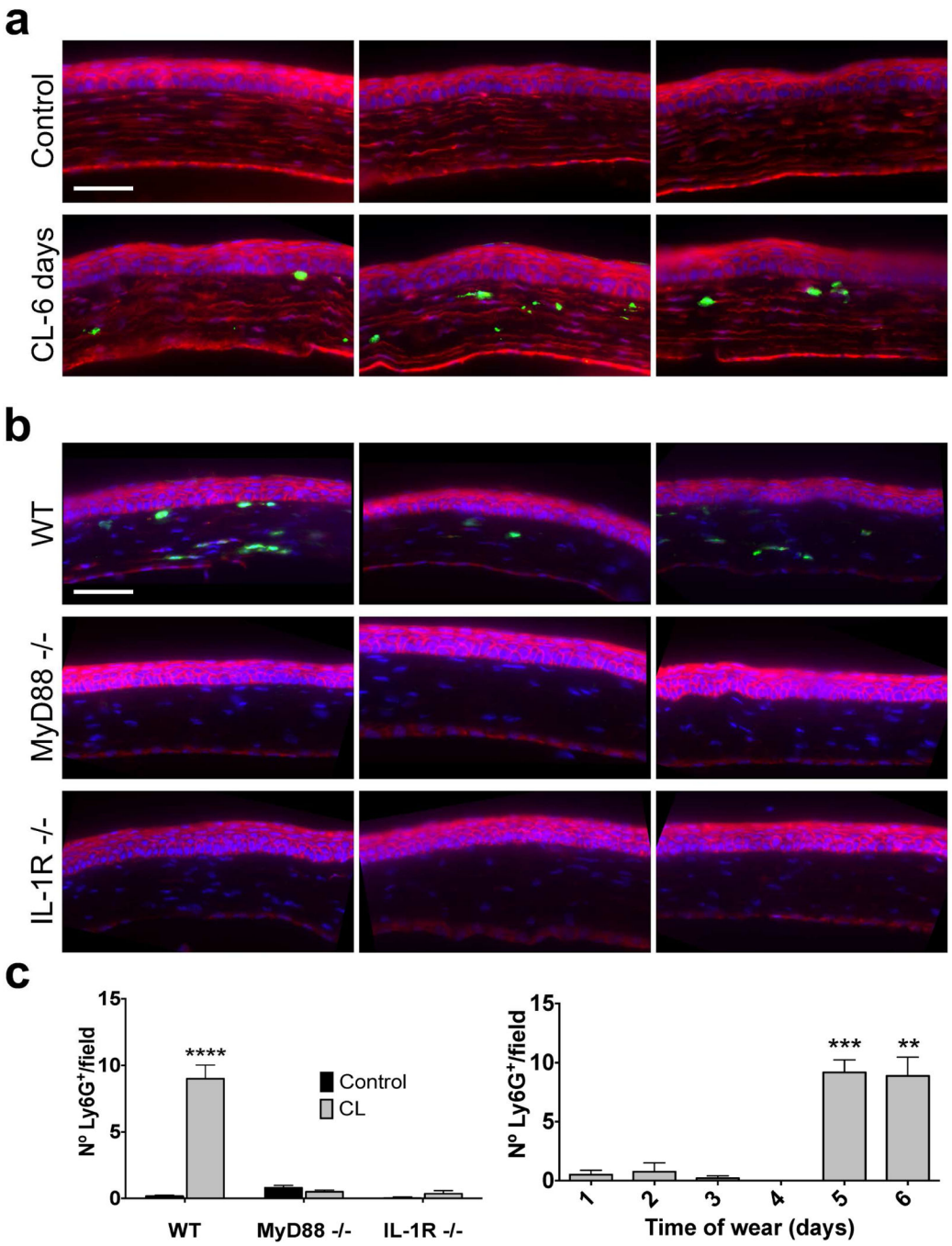

Fig. 5.

Immunofluorescence imaging showing neutrophil infiltration of contact lens wearing murine corneas after 6 days that requires MyD88 and IL-1R. (a) Cryo-sections of mT/mG mouse corneas (red, membrane) stained with DAPI (blue, nuclei) and Ly6G-antibody (green) showing $Ly6G^+$ cell (neutrophil) recruitment in the corneal stroma of lens-wearing eyes (6 days of continuous wear) compared to contralateral controls (3 different corneas are shown per group). (b) Cryo-sections of wild-type (WT), MyD88 (−/−), or IL-1R (−/−) murine corneas after 6 days of contact lens wear, stained with phalloidin (magenta, actin), DAPI

(blue, nuclei) and Ly6Gantibody (green) showing the absence of Ly6G-positive cells (neutrophils) in the gene-knockout corneas (3 different corneas shown per group). Scale bar = 50 μm. (c) Quantification of $Ly6G^+$ cells (neutrophils) (number of $Ly6G^+$ cells per field of view) in WT versus MyD88 (−/−) and IL1R (−/−) contact lens-wearing corneas versus controls (6 days lens wear) (left panel), and in WT mice at different time points after lens fitting (right panel). $Ly6G^+$ cell recruitment required 5 days of lens wear (**** $p < 0.0001$, *** $p < 0.001$, ** $p < 0.01$, Kruskal-Wallis test).

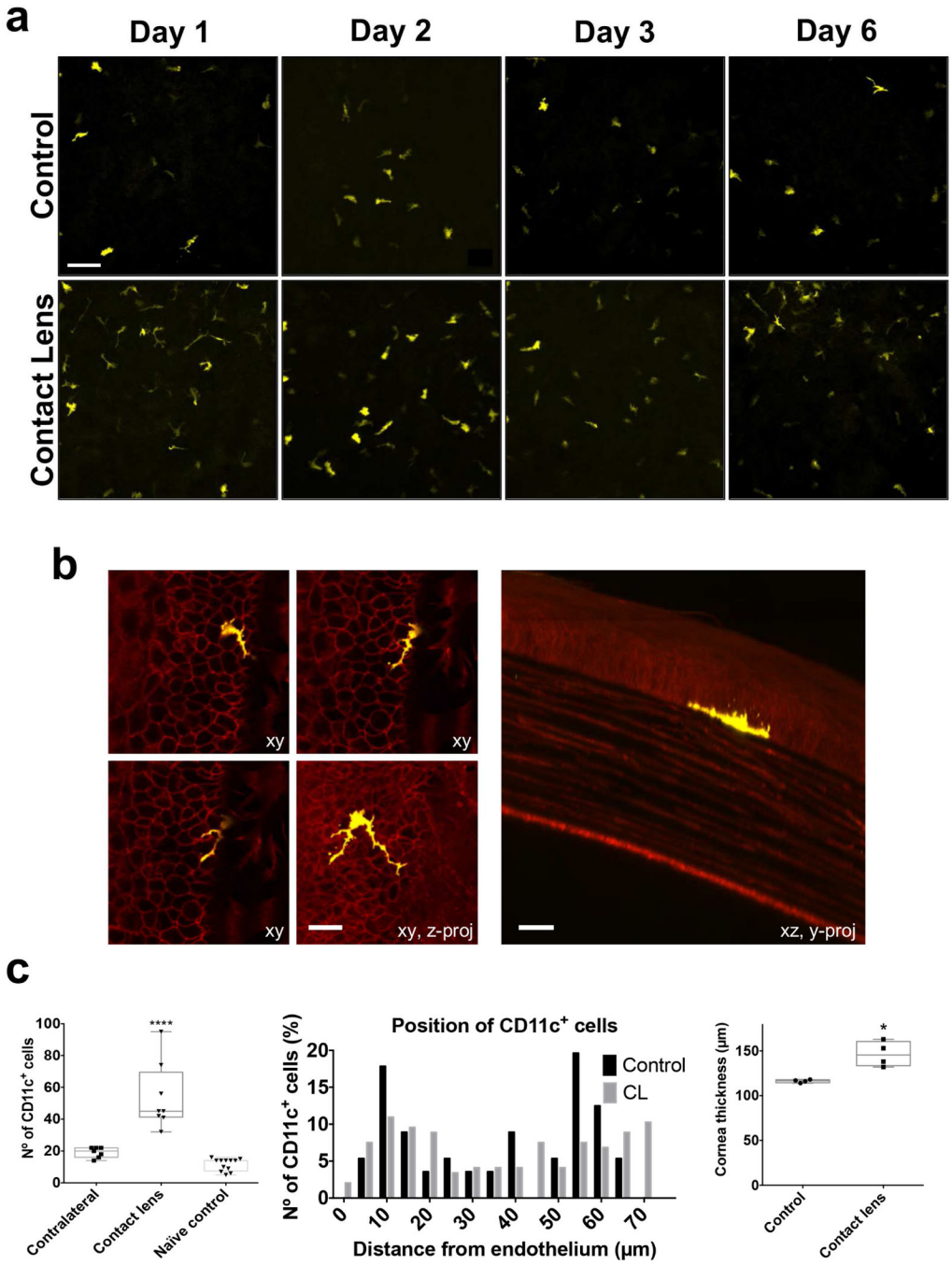

Fig. 6.

Early recruitment of CD11c$^+$ cells after contact lens wear. (a) Maximum intensity z-projection of the YFP signal (all CD11c$^+$ cells projected into one plane) in the central cornea of a contact lens-wearing eye shows an increased number of cells present versus the contralateral control at all time-points starting at 1 day. (b) Optical ortho-slicing (xy, 0.5 µm thick), maximum intensity z-projection (xy, z-proj, 24 µm thick) and maximum intensity y-projection (xz, y-proj) of a single CD11c$^+$ cell showing localization at, and across, the basal lamina with processes extending into the corneal epithelium after 6 days of contact lens

wear. (c) Quantification of the increase in $CD11c^+$ cells in the central cornea of lens-wearing eyes versus contralateral and naïve controls after 1 day (left graph, **** $p < 0.0001$, Kruskal-Wallis test), along with the distribution of $CD11c^+$ cells within the cornea (central graph) showing an increase in cell frequency closer to the endothelium and the epithelium versus contralateral controls, and increased corneal thickness in contact lens wearing eyes versus contralateral controls (right graph, * $p < 0.05$, unpaired Student's t-test).

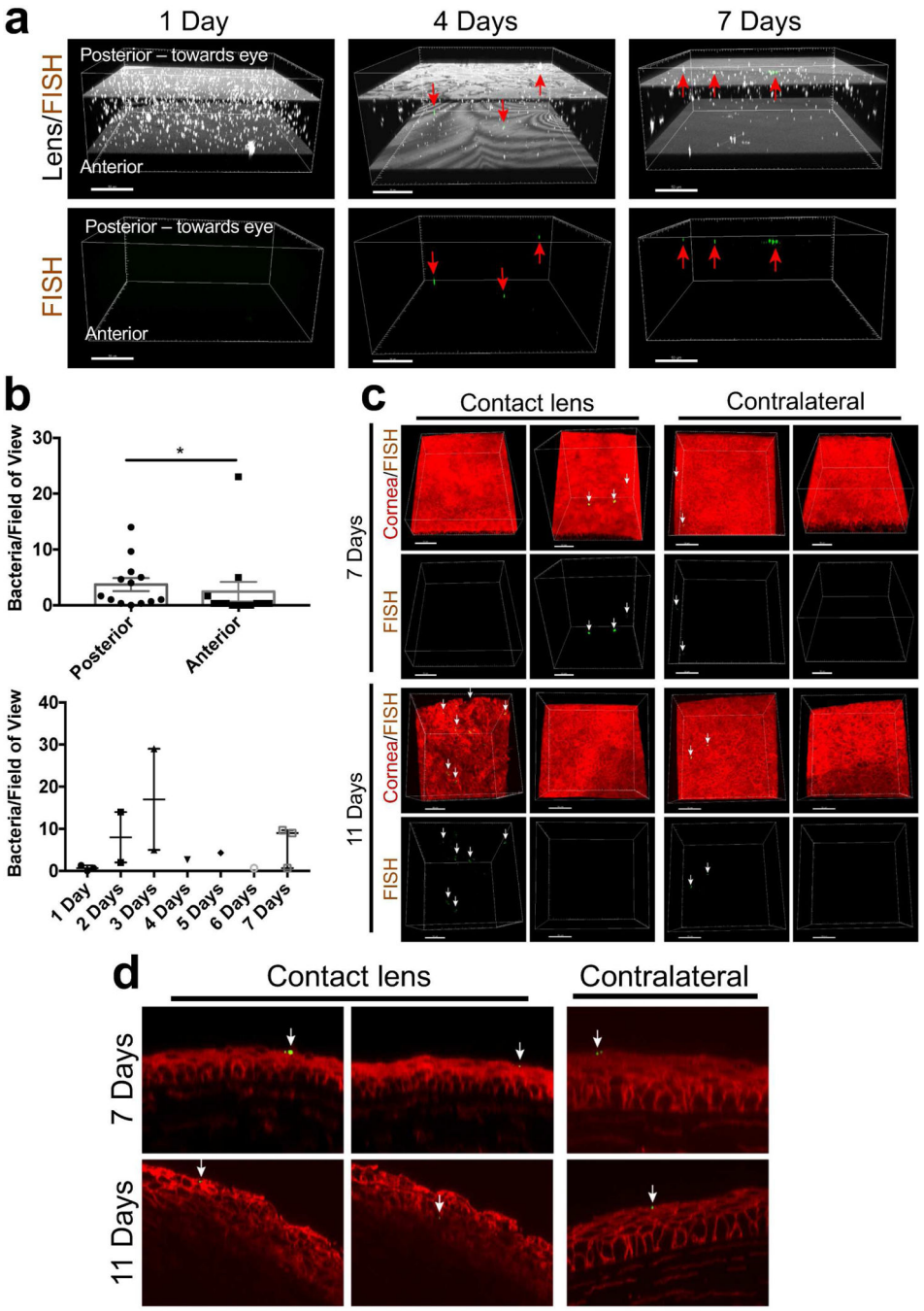

Fig. 7.

Colonization of murine contact lenses during wear by commensal bacteria. (a) FISH labeling using a universal bacterial 16S rRNA gene probe identified bacteria (red arrows) present on worn contact lenses at various time points. Bacteria were rarely identified on lenses worn for 1 day while several bacteria were identified on lenses at later time points. Bacteria were found on both the posterior and anterior lens surfaces. (b) Number of bacteria identified/field of view on the inside (posterior surface) of the worn contact lens compared to bacteria identified on the outside (anterior surface) (upper panel). Data expressed as a median with

interquartile range. (* p = 0.03, Mann-Whitney U Test). Number of bacteria identified in a field of view on worn contact lenses over time (lower panel). c) FISH labeling using a universal bacterial 16S rRNA gene probe on murine corneas after 7 and 11 days of contact lens wear. Very few viable bacteria were detected (white arrows) in contact lens wearing eyes or contralateral controls. (d) In rare instances, bacteria were also found within the corneal epithelium after 11 days of contact lens wear.

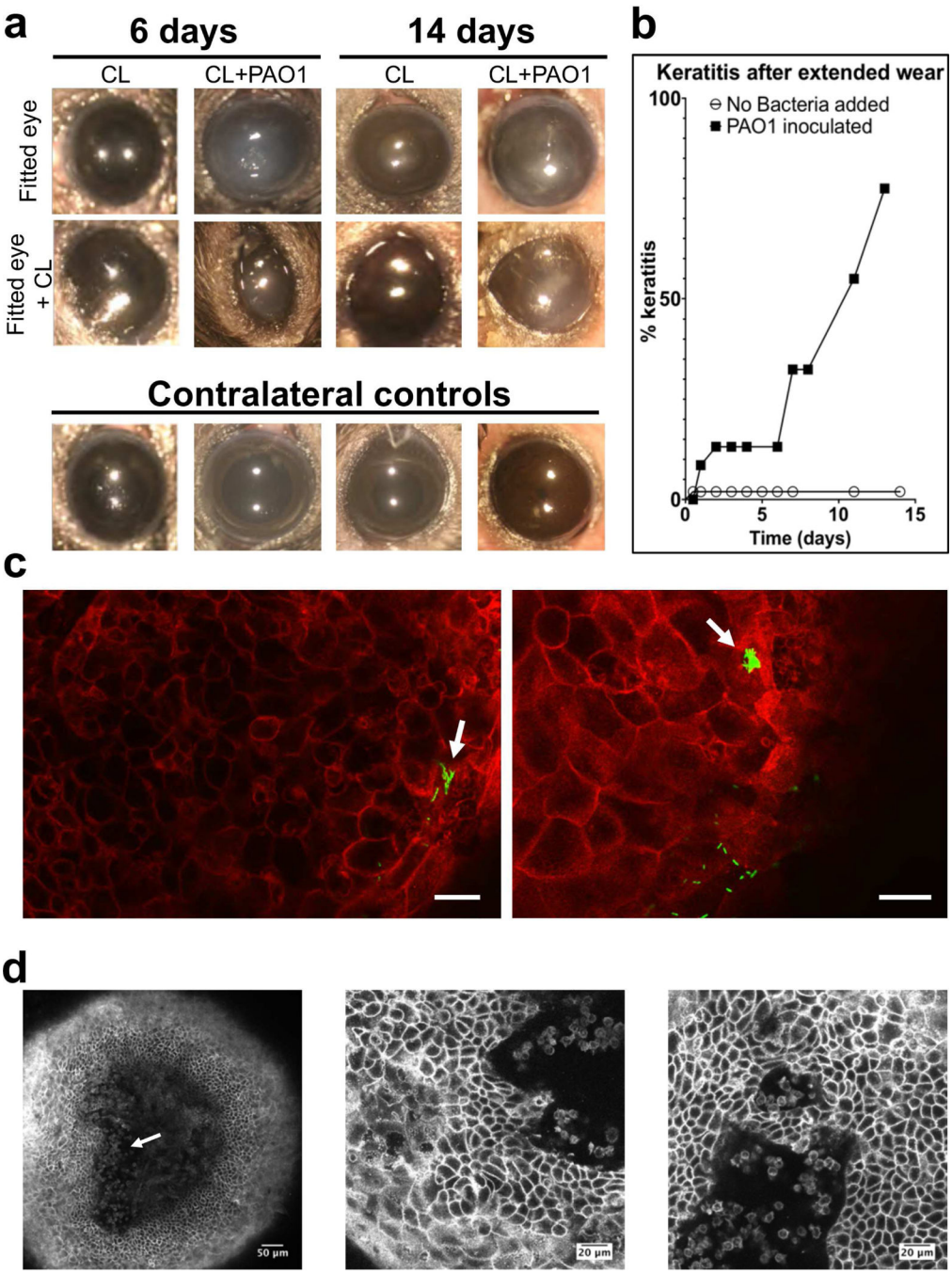

Fig. 8.

Development of microbial keratitis after fitting murine corneas with *P. aeruginosa* inoculated lenses. (a) *In vivo* images of mouse eyes wearing a contact lens (central row) previously inoculated with *P. aeruginosa* PAO1 (CL+PAO1) or not inoculated (CL), after removing the contact lens (top row) and contralateral controls (not fitted with a contact lens and not inoculated, bottom row) were taken using a dissecting microscope at indicated time points. Cornea opacity was present only in bacteria inoculated-contact lens wearing eyes. (b) Survival analysis showing the incidence of microbial keratitis in inoculated versus un-

inoculated contact lenses (keratitis was indicated by the presence of corneal opacity) ($p < 0.01$, Log-rank Mantel-Cox test). (c) Optical ortho-slicing (xy plane) of a mT/mG mouse cornea after 7 days wear of a PAO1-GFP inoculated contact lens showing an example of bacteria closely adherent to the surface, penetrating the disorganized epithelium and forming intra-tissue microcolonies (arrows). Green, bacteria and red, td-tomato cell membrane, scale bars = 20 μm. (d) Optical ortho-slicing (xy plane) of a mT/mG mouse cornea after 14 days wear of PAO1-inoculated contact lens showing an example of small round cells (resembling neutrophils) infiltrating and disrupting organization of the stroma in the central cornea (arrow, left image), and penetrating the corneal epithelium (central and right images).

Table 1.

Identification and quantification of bacteria on contact lenses worn by wild-type mice

Lens #	Days worn	CFU/Lens	Bacteria identified
1	1	10	*Staphylococcus* spp. (CNS)
2	1	10	*Bacillus* spp.
3	1	330 10 30	*Propionibacterium* spp. *Staphylococcus spp.* (CNS) *Actinobacillus spp.*
4	2	1935	*Corynebacterium* spp.
5	2	5120	*Corynebacterium* spp.
6	3	21500 370	*Staphylococcus* spp. (CNS) *Streptococcus* spp.
7	3	10	*Corynebacterium* spp.
8	4	1650	*Corynebacterium* spp.
9*	5	1500 10 10	*Corynebacterium* spp. *Staphylococcus* spp. (CNS) *Actinobacillus* spp.
10*	6	0	N/A
11*	7	41000	*Corynebacterium* spp.
12*	7	4900	*Corynebacterium* spp.
13	7	110 10	*Corynebacterium* spp. *Pseudomonas* spp.
14*	11	3330	*Corynebacterium* spp.

* Corneas were also examined for, and demonstrated, Ly6G-positive cell infiltration